Thermochimica Acta, 232 (1994) 233–242
Elsevier Science B.V., Amsterdam
SSDI 0040-6031(93)01387-I

Influence of morphology on textural properties and on the reactivity of chromium oxides obtained by decomposition of oxalate precursors $(NH_4)_3[Cr(C_2O_4)_3]$

A. Lerch and A. Rousset *

Laboratorie de Chimie des Matériaux Inorganiques, U.R.A. CNRS 1311, 118 Route de Narbonne, Université Paul Sabatier, 30162 Toulouse Cedex (France)

(Received 3 May 1993; accepted 2 June 1993)

Abstract

This article first describes a method of obtaining a chromium oxalate complex $(NH_4)_3[Cr(C_2O_4)_3]$ with extremely variable grain morphology (needles, polyhedra, platelets, spheres). The decomposition of these salts at 350°C in air leads to nonstoichiometric chromium oxides amorphous to X-rays, of composition CrO_x where x is close to 1.9.

The various oxides obtained at 350°C had very high specific surface areas of the order of several hundreds of $m^2\,g^{-1}$ which varied considerably according to the grain morphology. They all possessed a significant mesopore area with pores centred around 5 nm.

The crystallization of $CrO_{1.9}$ into α-Cr_2O_3 occurred on raising the temperature above 350°C and was accompanied by an emission of oxygen which took place in two stages. The kinetics of the oxygen emission varied with the grain morphology and could be correlated with the differences in length of the oxygen diffusion path corresponding to each oxide form.

INTRODUCTION

Like the majority of transition-metal oxides, the oxides of chromium possess interesting physicochemical properties not only from a fundamental point of view, but also from that of their applications. Thus CrO_2 is used for high density magnetic recording, whilst the oxide Cr_2O_3 enters the composition of many catalysts [1,2].

Moreover, it has been firmly established that the methods of preparation play a very important role in the properties of solids, especially when these involve compounds obtained at low temperatures. In such conditions, it is possible to prepare the solids with controlled morphology and thus to control a certain number of physical and chemical properties (reactivity, catalysis, etc.).

As far as chromium oxides are concerned, the majority of earlier studies

---

* Corresponding author.

have involved preparative methods concerning the decomposition of hydroxides or gels [3, 4]. Our own interest has been in other precursors, in particular oxalate complexes of general formula $(NH_4)_3[Cr(C_2O_4)_3] \cdot 3H_2O$, which have until now been much less studied for obtaining chromium oxides.

In this article, we show that it is possible to obtain these precursors with different morphologies and that their decomposition can lead to metastable and nonstoichiometric oxides whose textural characteristics can vary within quite wide limits.

MEASUREMENTS

Microscopic observations were carried out with a Cambridge Stereoscan 250MK3 microscope.

Measurements of specific surface areas and pore volumes were carried out with a Coultronics automatic apparatus Model Accursorb 2100E, controlled by a Hewlett-Packard HP86B computer. Before every analysis the samples were degassed under primary vacuum at 200°C. The surface area S_{BET} was calculated by applying the conventional BET equation to the initial regions of the absorption isotherms (0.05–0.3 P_s) where P_s is the saturation pressure. The pore size distribution was calculated from the nitrogen isotherms by the method of Barrett, Joyner and Haleda [5], which also permits the calculation of cumulative pore volume.

The thermogravimetric curves were recorded on a Setaram thermoanalyzer, operating under a current of air and argon gas. The gas circulation rate was calculated to be $1.5\ \mathrm{l/h^{-1}}$. The rate of temperature rise corresponded to $3°\mathrm{C\ min^{-1}}$ for treatments under air and $5°\mathrm{C\ min^{-1}}$, 50 mg sampling and references, using a reference made up of corundum, $\alpha\,Al_2O_3$.

RESULTS AND DISCUSSION

Preparation and characterization of oxalate precursors

The conditions for obtaining chromium(III) oxalate in aqueous media have already been described [6, 7]. Recently Devaux [8] has shown that by precipitation in alcohol it is possible to obtain anhydrous salts with a more regular morphology than those obtained by evaporation of solvents. Thus the chromium oxalate complex $(NH_4)_3[Cr(C_2O_4)_3]$ was prepared by mixing ammonium oxalate (3 M) and a chromium(III) salt ($Cr(NO_3)_3 \cdot 9H_2O$ (1 M) in aqueous media with heating (60°C). The clear solution was cooled, then added rapidly to a mixture of two solvents where precipitation occurred immediately.

TABLE 1

Preparative conditions for oxalate complexes

Sample number	% and nature of 1st solvent	% and nature of 2nd solvent	Grain shape	Average grain size from SEM
1	50 ACET	50 MET	Needles	100 ± 30
2	13 ACET	87 ETG	Platelets	80 ± 20
3	60 ACET	40 ETG	Spheres	40 ± 10
4	50 ETH	50 ETG	Polyhedra	20 ± 5

Key: ACET, acetone; ETG, ethylene glycol; ETH, ethanol; MET, methanol.

In an attempt to control the grain morphology, we used different precipitation parameters, chiefly the nature of the solvents. The conditions used and the results obtained by scanning microscopy are listed in Table 1 and Fig. 1.

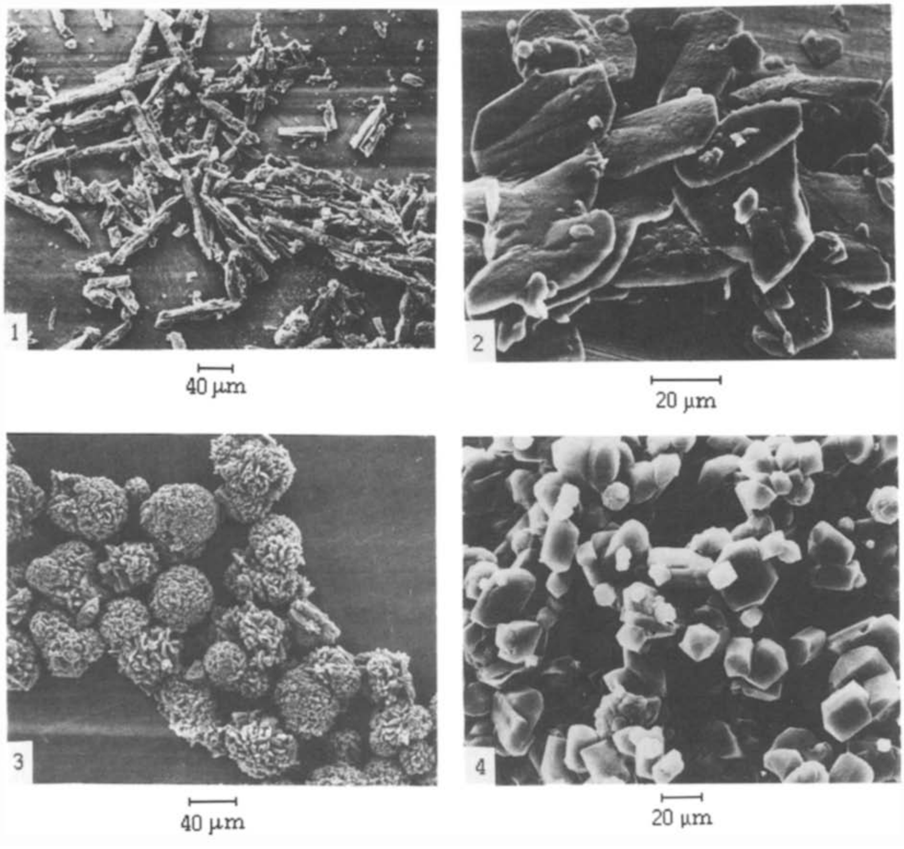

Fig. 1. Micrographs of chromium oxalate with different morphologies.

The oxalates corresponding to samples 1, 2 and 4 were made up of monolithic grains; in contrast sample 3 was made up of aggregates of platelets of small dimensions (4–5 μm).

Decomposition of the oxalic precursor $(NH_4)_3[Cr(C_2O_4)_3]$ in air and characterization of oxides obtained

The decomposition in air of the preceding oxalic precursors followed by thermogravimetric analysis gave identical results whatever the grain morphology. No loss in mass was apparent between 100 and 150°C, thus confirming the anydrous character of the salts.

As shown by the thermogravimetric curve represented in Fig. 2, the trioxalate chromium complex decomposes between 250 and 350°C. However, although the majority of the mass loss occurs at the latter temperature (97.5%), there also appears to be a small loss of around 2.5% between 350 and 400°C.

Below 400°C no mass loss was apparent, and radiocrystallographic analysis indicated the presence of αCr_2O_3 with the temperature of crystallization, determined by calorimetry, at around 380°C.

The phases obtained at 350°C were, however, completely devoid of all crystalline organization (X-ray diagram devoid of lines or diffraction halos) and their chemical analysis showed the presence of small quantities of nitrogen (0.1 mass%) and carbon (0.2 mass%). These badly organized solids contain high proportions of chromium(VI) as shown by chemical analysis (determination by ferrous salt) and by ESCA. Taking account of

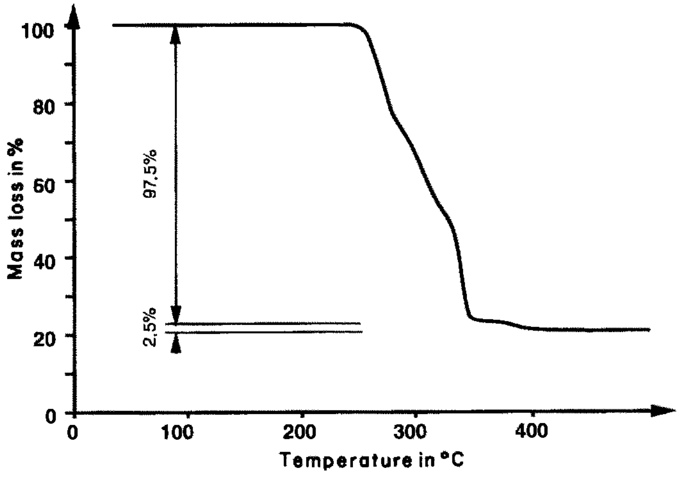

Fig. 2. Thermogravimetric curve of chromium oxalate with polyhedral grain shape.

TABLE 2

Textural characteristics of CrO_x oxides

Parameter [a]	Needles	Polyhedra	Platelets	Spheres
S_w in $m^2\,g^{-1}$	350	254	241	206
V_p in $cm^3\,g^{-1}$	0.193	0.102	0.078	0.131
V_m in $cm^3\,g^{-1}$	0.097	0.094	0.066	0.116

[a] S_w = specific surface area, V_p = total pore volume, V_m = mesopore volume; $\Phi < 20$ nm.

the mass loss recorder between 350 and 400°C, and allowing that this loss is essentially due to oxygen, it could also be due to nonstoichiometric oxides of chromium of the type CrO_x where x is between 1.5 and 2.

Texture of CrO_x ($1.5 < x < 2$)

All the oxides obtained at 350°C had very high specific surface areas (Table 2) which varied considerably according to the particle morphology.

The nitrogen adsorption isotherms recorded for each oxide correspond to the classical curves for which the penetration by nitrogen molecules occurs progressively as a function of partial pressure. During desorption, the hysteresis cycles found are identical to the type B curve of De Boer's classification [9], characteristic of a capillary adsorption of slit shape type.

Curves of cumulative volumes (Fig. 3) and of pore size distribution according to pore diameter, were drawn for oxides with different morphologies and showed all the samples to be made up of a major proportion of mesopores centred around 5 nm, surrounded by a low proportion of macropores. However the quantity of mesopores varied significantly according to the oxide morphology (Table 2). Thus the oxides

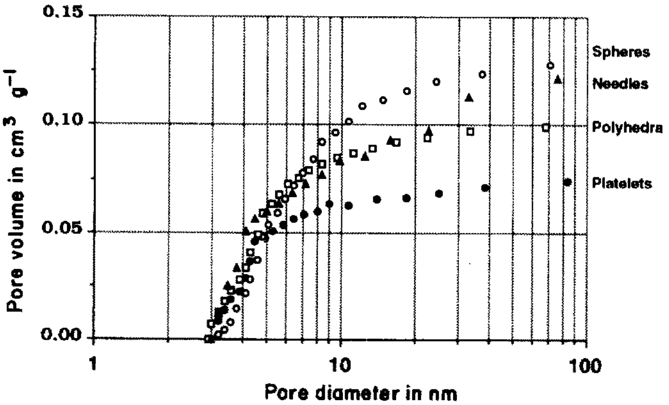

Fig. 3. Pore volume as function of pore diameter for different oxides with variable grain shape.

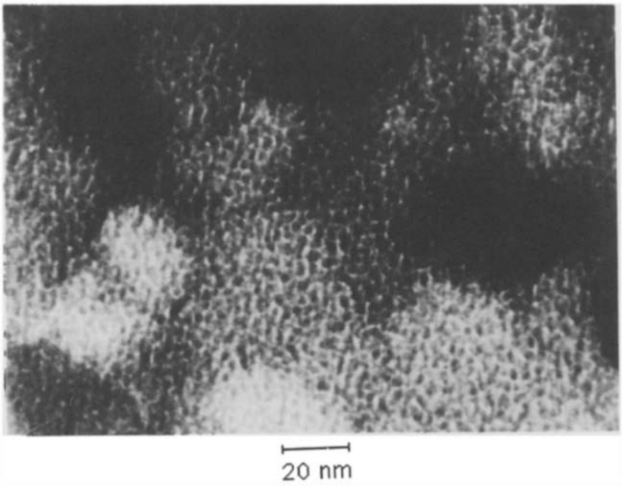

Fig. 4. Micrograph of chromium oxide with polyhedral shape.

with spherical grains had a significant mesopore volume compared with the other oxides.

We noted in addition the appearance of a large-diameter porosity (>20 nm) for those oxides with needle-shaped grains. The pore distribution was thus very spread out. In contrast, the other oxides showed a much narrower pore distribution.

Electron microscopy confirmed and completed the foregoing observations. Figure 4 shows that the oxide with polyhedral grains is made up of very tiny crystallites ($\Phi \approx 4$ nm) separated by intervals of small dimension, the area of mesoporosity. The pores occupying the spaces between the grains are slit-shaped, which is in agreement with the results obtained from the adsorption-desorption isotherms.

The theoretical specific surface area ($270\,\mathrm{m}^2\,\mathrm{g}^{-1}$) determined from crystallite size is close to that obtained by the BET method ($254\,\mathrm{m}^2\,\mathrm{g}^{-1}$).

Changes in CrO_x oxides with temperature

The study of the mass loss occurring between 350 and 400°C was made with great precision by thermogravimetric analyses of the relatively major amounts of CrO_x oxide obtained at 350°C in air.

The curves obtained for each grain morphology are shown in Fig. 5. They reveal that at low temperature there is a major mass loss related to the strong water adsorption, as usually occurs with very divided solids. This mass loss is followed by another more rapid loss, which represents the change of CrO_x into Cr_2O_3 with much greather sensitivity. This loss, of the order of 7% compared with the initial oxide mass, should correspond

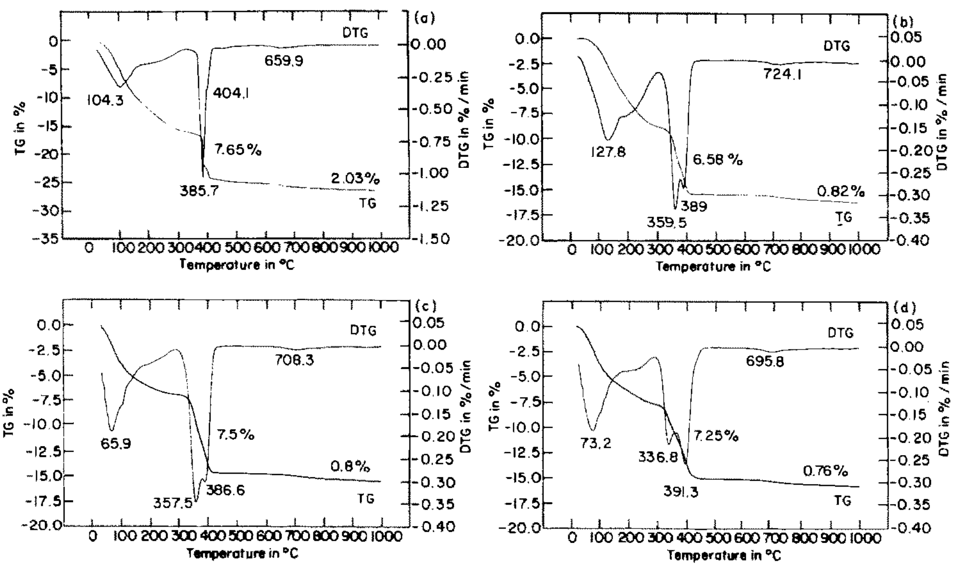

Fig. 5. Thermogravimetric curves of oxide $CrO_{1.9}$ obtained at 350°C under air with (a) polyhedral shape, (b) needle shape, (c) spherical shape, (d) platelet shape.

essentially to a loss of oxygen, according to the previously proposed hypothesis.

This hypothesis has been effectively confirmed by coupling the thermogravimetric analysis to a mass spectrometer under argon. The spectrum obtained (Fig. 6) demonstrates an oxygen loss between 350 and 450°C which occurs in two stages, as had predicted by the DTG curves of Fig. 5. This phenomenon is accompanied by a loss of adsorption water which is

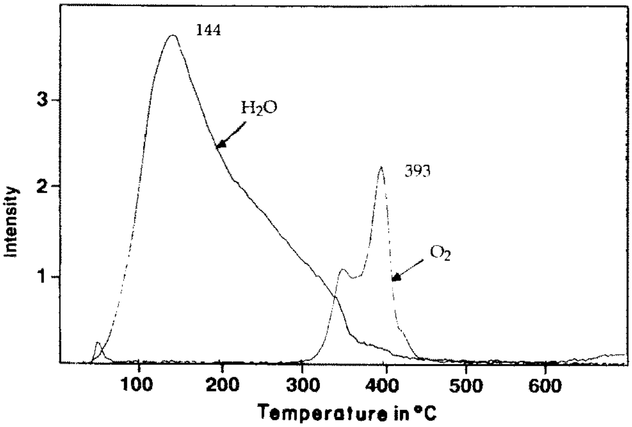

Fig. 6. Curve obtained by mass spectrometer of chromium oxide with spherical shape under argon.

TABLE 3

Temperatures corresponding to the two oxygen losses

Peak temperature/°C	Spheres	Needles	Platelets	Polyhedra
Lowest	337	357	359	386
Highest	391	389	389	404
Difference between two temperatures	54	32	30	18

effectively removed between 100 and 300°C. However it is only above 700°C that the $CrO_{1.5}$ stoichiometry is finally established, as shown by the DTG curves.

Thus those oxides produced immediately at the end of the decomposition in air of the $(NH_4)_3[Cr(C_2O_4)_3]$ complex are amorphous, nonstoichiometric, and correspond to the general formula CrO_x where x is around 1.9. Raising the temperature above 350°C causes the oxides to lose their excess of oxygen to approach progressively the composition corresponding to $CrO_{1.5}(Cr_2O_3)$ and simultaneously crystallize in a corundum network (αCr_2O_3). The oxygen loss generally takes place in two stages with a similarity in the behaviour for needle-shaped or platelet-shaped grains (DTG curves, Fig. 5(b), (c)). However, the temperature at which oxygen loss begins is the lowest for spherical grains and highest for those which are polyhedral-shaped, with much more rapid kinetics in the latter case (Table 3, Fig. 5(a), (d)).

Study of the transformation of CrO_x into Cr_2O_3

The study of the kinetics of crystallization is based on Kissinger's theory [10]. Analysis was carried out in non-isothermic mode and utilized the displacement of the crystallization peak as a function of the rate of heating. The activation energy of crystallization (E) can be deduced from the slope on the straight line

$$\ln(a/T_m^2) = f(1/T_m) \qquad (1)$$

where a is the rate of temperature rise and T_m is the temperature corresponding to the peak signal.

In all cases, the CrO_x oxides ($x \approx 1.9$) obtained at 350°C in air are shown in calorimetric analysis to produce an acute exothermic phenomenon around 380°C. This phenomenon occurs simultaneously with the oxygen loss and corresponds to the crystallization of the amorphous oxide to αCr_2O_3.

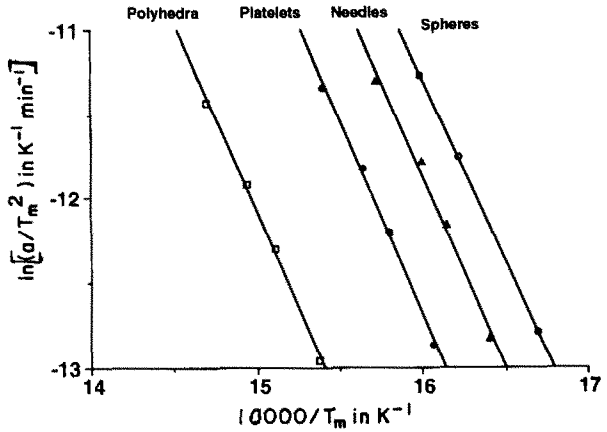

Fig. 7. Ln(a/T_m^2) as function of 10 000/T_m for oxides with different morphologies.

Figure 7 represents the straight lines corresponding to eqn. (1) described above for the $CrO_{1.9}$ oxides of different morphologies. The straight lines are all displaced one from another, which would indicate that the crystallization temperature is a function of the grain geometry. The grain size, however, cannot be directly correlated with the crystallization temperature. We can thus classify crystallization temperatures according to the grain form, as follows:

T_m(polyhedra) > T_m(platelets) > T_m(needles) > T_m(spheres)

The activation energies of crystallization determined by the slopes of the straight lines of Fig. 7 are very close whatever the form, size, surface area and pore volume of the oxide studied (Table 4). It thus seems that these parameters, and in particular the form of the elementary grains, favourably influence the transformation kinetics (crystallization + oxygen elimination) more than the energies involved.

It is necessary to remember that the spherical particles are made up of very small (a few microns) elementary gain agglomerates with the dimensions of the other particles. Under these conditions it would therefore seem logical that the transformation of amorphous $CrO_x \rightarrow \alpha Cr_2O_3$ should be the most rapid considering the relatively short distances of the oxygen diffusion paths. Conversely, in the much more voluminous polyhedral

TABLE 4

Activation energy of crystallization of CrO_x oxides

	Spheres	Needles	Platelets	Polyhedra
E in kcal mol^{-1}	42 ± 2	44 ± 2	45 ± 2	44 ± 2

particles, the lengths of the oxygen diffusion paths are much greater and the crystallization temperatures significantly higher.

As far as the particles in the shape of needles and platelets are concerned they show related behaviour (ATG and DTG curves), which could be explained by the fact that their thickness is relatively small and is closer to the dimensions of the elementary grains made up of spherical particles than those of the approximately isotropic polyhedral particles (20 m).

CONCLUSIONS

The decomposition of the oxalate complexe salts $(NH_4)_3[Cr(C_2O_4)_3]$ at 350°C leads to amorphous nonstoichiometric metastable oxides corresponding to a general formula close to and strongly dependent on the morphology of the precursor particles. These oxides can be transformed into Cr_2O_3 by raising the temperature, and elimination of the excess oxygen ($CrO_{1.9} \rightarrow CrO_{1.5}$) generally takes place in two stages. The activation energy of this transformation is not dependent on the particle form. The transformation temperature is highest for the large diameter isotropic particles, and lowest for the needles or platelets of small thickness. Under these conditions, it then seemed logical to correlate the length of the oxygen diffusion path and thus the reactivity of these solids with the shape of their component particles.

ACKNOWLEDGEMENT

The authors express their sincere thanks to Mr. A. Lantz and Mr. E. Lacroix of the society Atochem for their suggestions and stimulating discussions.

REFERENCES

1 R.L. Burwell, G.L. Haber, K.C. Taylor and J.F. Read, Adv. Catal., 29 (1969) 1.
2 H.E. Curry-Hyde, H. Musch and A. Baiker, Ind. Eng. Chem. Res., 29 (1990) 1985.
3 J. Fenerty and K.S.W. Sing, Proc. 1st Eur. Symp. Therm. Anal., (1976) 305.
4 W. Weller and S.E. Voltz, J. Am. Chem. Soc., 76 (1954) 4695.
5 E.P. Barrett, L.C. Joyner and P.P. Haleda, J. Am. Chem. Soc., 73 (1951) 373.
6 J. Pâris, A. Rousset and F. Chassagneux, in C. Eyraud and M. Escoubes (Eds.), Progress in Vacuum Microbalance Techniques, Vol. 3, Heyden, London, 1975, p. 416.
7 A. Rousset, J. Pâris and J. Comes, Bull. Soc. Chim. Fr., 2 (1969) 446.
8 X. Devaux and A. Rousset, French Patent No. 9009790, 24-07-1990.
9 J.H. De Boer, The Structure and Properties of Porous Materials, Butterworths, London, 1970, p. 123.
10 H.E. Kissinger, J. Res. NBQ, 57 (1956) 217.